



Scholars Research Library

Der Pharma Chemica, 2015, 7(1):84-91
(<http://derpharmachemica.com/archive.html>)



ISSN 0975-413X
CODEN (USA): PCHHAX

Tuning structural stability and electronic properties of MnSe nanostructures – a DFT study

V. Nagarajan, V. Saravanakannan and R. Chandiramouli*

School of Electrical & Electronics Engineering, SASTRA University, Tirumalaisamudram, Thanjavur, India

ABSTRACT

The realistic nanostructures of pure, Cr and Te substituted MnSe nanostructures are simulated successfully using density functional theory with B3LYP/ LanL2DZ basis set. Using calculated energy and chemical hardness, structural stability of MnSe nanostructures are discussed. Dipole moment and point symmetry of pure, Cr and Te substituted MnSe nanostructures are also studied. The electronic properties of MnSe nanostructures are discussed in terms of electron affinity, ionization potential and HOMO-LUMO gap. The present work provides the information for tailoring MnSe nanostructures with the incorporation of impurities to improve the structural stability and electronic properties, which finds its application in spintronic devices, solar cells and electrocatalysts.

Keywords: manganese selenide; nanostructures; dipole moment; electron affinity; chemical hardness

INTRODUCTION

Transition-metal chalcogenides are represented as MX_n , (M = transition metal; X=S, Te and Se) which are more extensively investigated owing to their magnetic, electrical and optical properties [1-3]. During synthesis of nanostructures, controlling the size and shape of crystallite is a critical task in order to tailor their properties with enhanced performance in wide range of applications such as spintronic devices [4], solar cells [5], electrocatalysts [6] and biological labelling [7]. Thus, preparing anisotropic chalcogenide semiconductor has its importance in modern technology and science. In recent days, research is concentrated on controlling the morphology of metal chalcogenide nanomaterials. Manganese selenide (MnSe) is one of the semiconductors due to strong electron interaction between hole/electron in sp-d band states which arise due to Mn^{2+} ions on Mn^{2+} 3d electron states [8]. MnSe exhibits cubic structure and hexagonal structure with lattice constant of ($a=5.462 \text{ \AA}$) and ($a=3.63 \text{ \AA}$; $c=5.91 \text{ \AA}$) respectively. MnSe becomes insulator at room temperature, which resemble NaCl type structure and it possess antiferromagnetic transition in the temperature range of 130 K to 250 K [9-11]. MnSe shows direct energy band gap in the range of 1.13 – 1.25 eV [12, 13]. MnSe is an important p-type semiconductor which shows various properties namely superconductivity, semiconductivity and magnetism [14]. Moreover, MnSe materials are used as dilute magnetic semiconductors, rechargeable battery electrodes, gas sensing, solar energy absorbers and electrochromic devices [15-17]. Various synthesis methods are employed to prepare MnSe nanostructures, which includes solution-phase hydrothermal route to synthesis nanorods [18], nanowires [19] and cube-like morphology are obtained by synthesizing MnSe using sonochemical method [20]. Bulk MnSe semiconductor has a wide band gap with the value of 2.65 eV, which possesses excellent transport, optoelectronic and magnetic properties. The inspiration behind this work is to tailor structural stability and electronic properties of MnSe nanostructures with substitution of Cr and Te atoms in order to improve its electronic properties. Density functional theory is a promising method to investigate the structural stability and electronic properties of MnSe nanostructures. In the present work, the structural stability and the electronic properties of impurity substituted MnSe nanostructures are studied and reported.

MATERIALS AND METHODS**Computational Methods**

The pure, Cr and Te substituted MnSe nanostructures in the form of nanotube and nanosheet are successfully optimized and simulated using Gaussian 09 package [21]. The atomic number of manganese and selenium is twenty five and thirty four respectively. In the present work, impurities are substituted in pure MnSe nanostructures and optimized. MnSe nanostructures are optimized with Becke's three-parameter hybrid functional (B3LYP) along with suitable LanL2DZ basis set [22-24]. While simulating MnSe nanostructures, choosing the basis set is an important criterion. Thus, LanL2DZ basis set is a good choice to optimize MnSe nanostructures with pseudo potential approximation [25]. Furthermore, this basis set is suitable for Hf-Bi, H and Li-La elements. The density of states (DOS) spectrum of MnSe nanostructures are drawn with the help of Gauss Sum 3.0 package [26].

RESULTS AND DISCUSSION

The present work, mainly concentrates on ionization potential (IP), dipole moment (DM), chemical potential (CP), chemical hardness (CH), calculated energy, electron affinity and HOMO-LUMO gap of MnSe nanostructures and the electronic properties of MnSe are fine-tuned with the substitution of dopant elements such as chromium and tellurium.

Figure 1 (a) – 1(c) represents pure, Cr and Te substituted MnSe nanosheet respectively. The intrinsic MnSe nanosheet consists of twelve Mn atoms and twelve Se atoms to form sheet like structure. Cr substituted MnSe nanosheet contains twelve Se atoms, nine Mn atoms and three Mn atoms are replaced with three equivalent Cr atoms. Te substituted MnSe nanosheet has twelve Mn atoms, nine Se atoms and three Se atoms are replaced with three Te atoms. Similarly, Figure 1 (d) – Figure 1 (f) depicts pure, Cr and Te substituted MnSe nanotube respectively. The intrinsic MnSe nanotube consists of twelve Mn atoms and twelve Se atoms. Cr substituted MnSe nanotube has twelve Se atoms, nine Mn atoms and three Mn atoms are replaced with three Cr atoms to form sheet like structure. Te substituted MnSe nanotube has twelve Mn atoms, nine Se atoms and three Se atoms are replaced with three Te atoms.

Figure 1(a). Structure of pure MnSe nanosheet

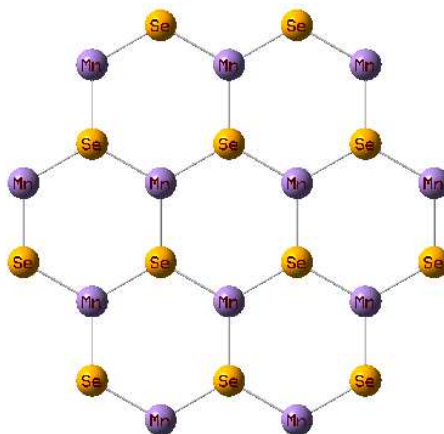


Figure 1(b). Structure of Cr substituted MnSe nanosheet

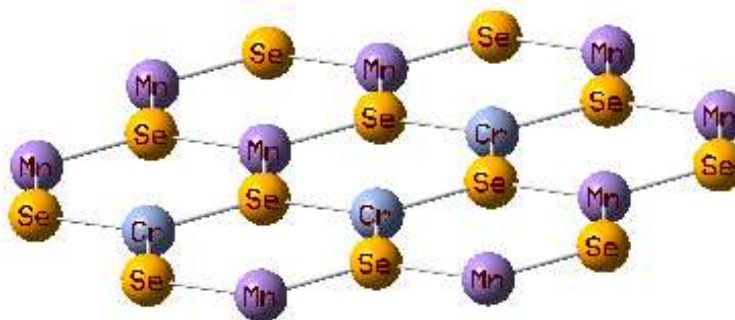


Figure 1(c). Structure of Te substituted MnSe nanosheet

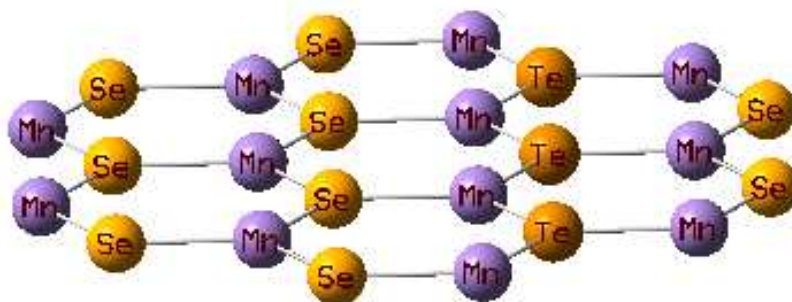


Figure 1(d). Structure of pure MnSe nanotube

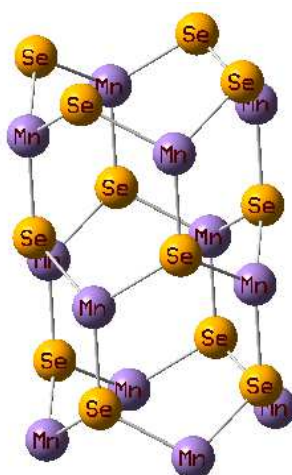


Figure 1(e). Structure of Cr substituted MnSe nanotube

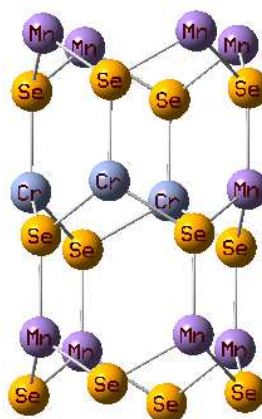


Figure 1(f). Structure of Te substituted MnSe nanotube

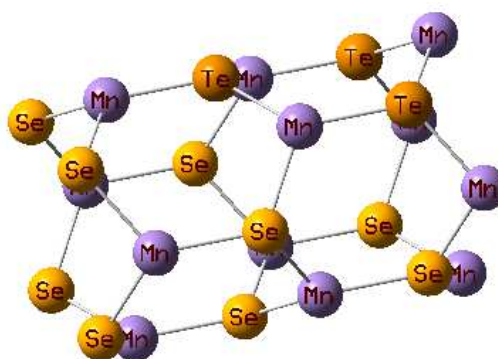


Table 1. Energy, point symmetry and dipole moment of MnSe nanostructures

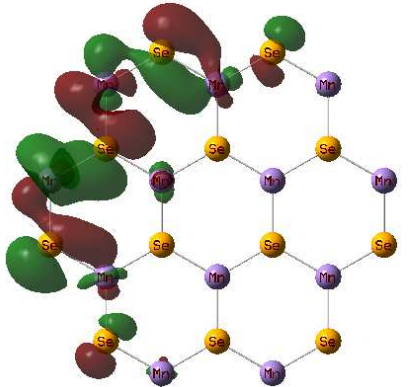
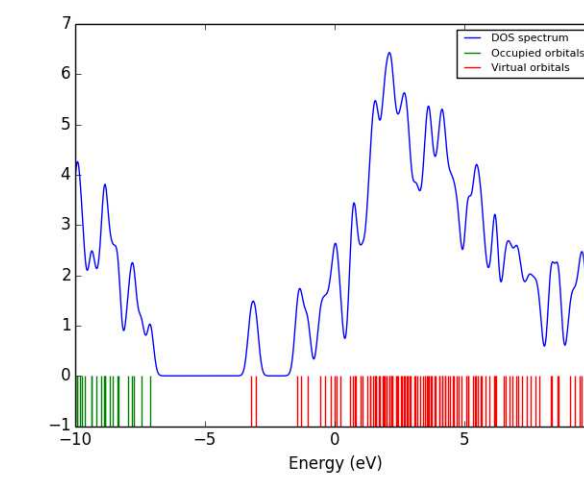
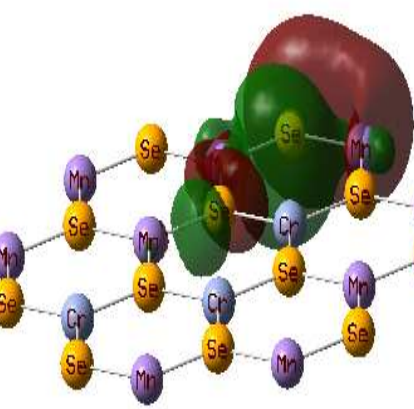
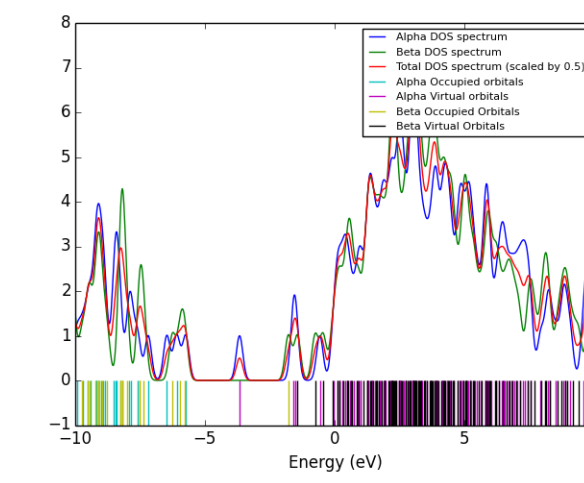
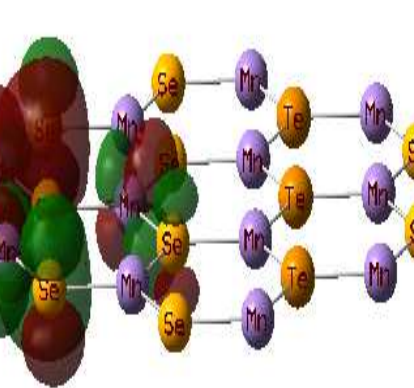
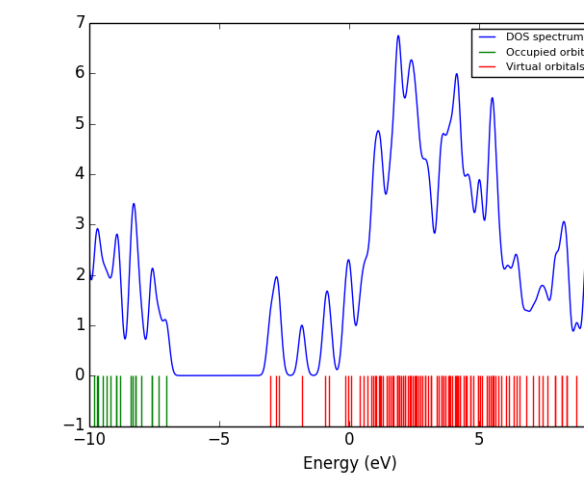
Nanostructures	Energy (Hartrees)	Dipole moment (Debye)	Point Group
Pure MnSe nanosheet	-1344.27	10.83	C _s
Cr substituted MnSe nanosheet	-1292.88	32.04	C _s
Te substituted MnSe nanosheet	-1340.55	1.57	C _s
Pure MnSe Nanotube	-1344.2	19.76	C _{4v}
Cr substituted MnSe nanotube	-1292.84	17.58	C _s
Te substituted MnSe nanotube	-1340.49	15.79	C _s

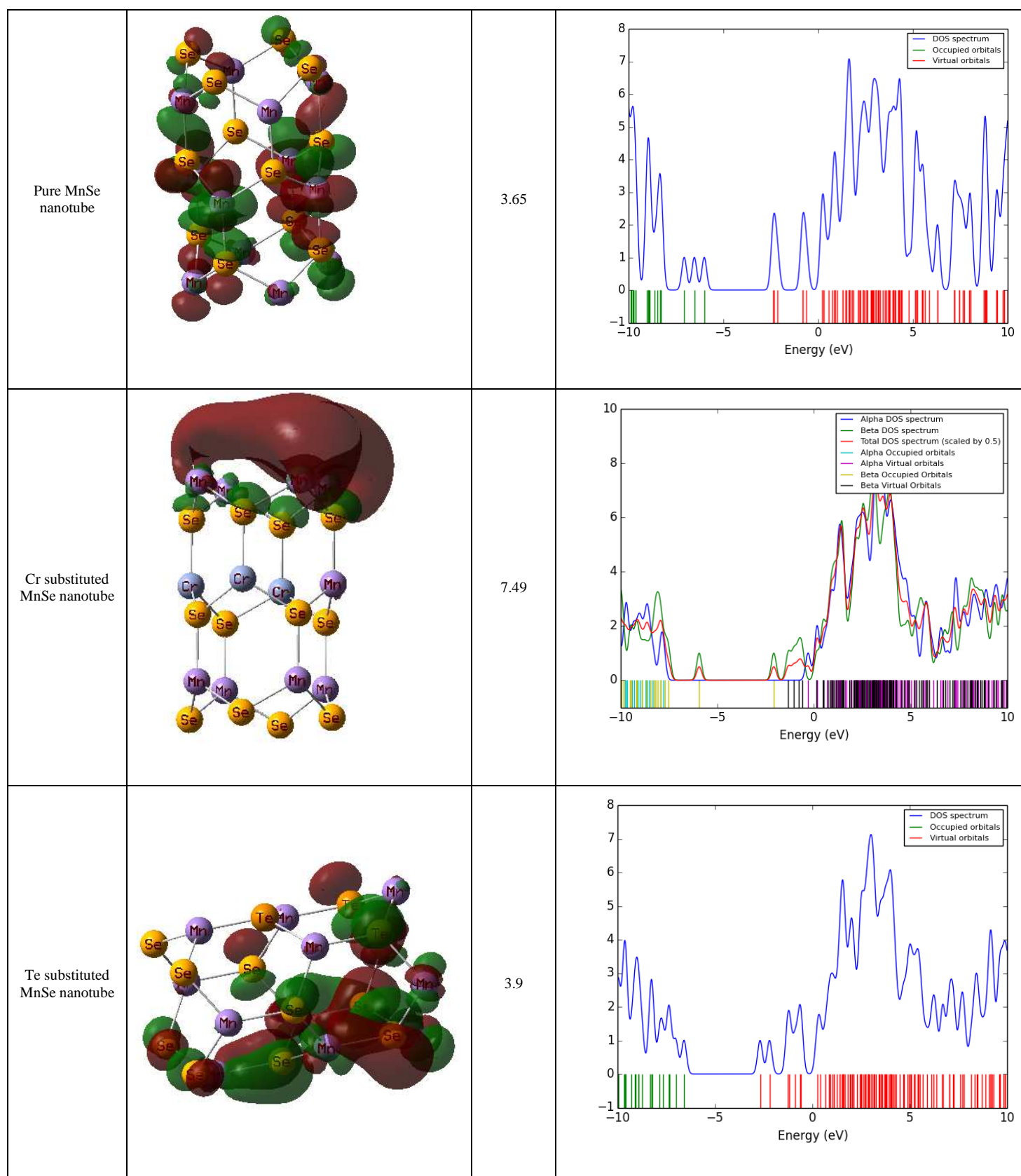
Structural stability of MnSe nanostructures can be discussed using calculated energy. The point group, calculated energy and dipole moment (DM) of pure, Cr and Te substituted MnSe nanostructures are tabulated in Table 1. The calculated energy of pure, Cr and Te substituted MnSe nanosheet are -1344.27, -1292.88 and -1340.55 Hartrees respectively. In that order, the calculated energy of pure, Cr and Te substituted MnSe nanotube are -1344.2, -1292.84 and -1340.49 Hartrees. The stability of MnSe nanostructure is directly proportional to the calculated energy. The pure MnSe nanosheet and nanotube have high value of calculated energy, the incorporation of impurities such as Cr and Te leads to decrease in the structural stability. Even though, the structural stability decreases for impurity substituted MnSe nanostructures; the electronic properties may be improved with the presence of impurity. The DP of pure, Cr and Te substituted MnSe nanosheet are 10.83, 32.04 and 1.57 Debye respectively. Similarly, the corresponding DP of pure, Cr and Te substituted MnSe nanostructures are 19.76, 17.58 and 15.79 Debye. From the observations, the DP value decreases with Te substitution in MnSe nanosheet. This refers that the charges present inside MnSe nanostructures are uniformly distributed with Te substitution compared with pure and Cr substituted MnSe nanostructures. The point symmetry group of pure MnSe nanotube is found to be C_{4v} and for the remaining MnSe nanostructures; all belongs to C_s which exhibits only one symmetry operation, identity operation E.

The electronic properties of MnSe nanostructures can be analyzed by lowest unoccupied molecular orbital (LUMO) and highest occupied molecular orbital (HOMO) [27-30]. The energy gap value for pure, Cr and Te substituted MnSe nanosheet and nanotube are tabulated in Table 2. From the observation of HOMO-LUMO gap, the substitution of dopant elements influence the energy gap compared with intrinsic or pure MnSe nanostructure. The energy gap value for pure, Cr and Te substituted MnSe nanostructure are 3.87, 2.07 and 4.01 eV respectively. This infers that the conductivity of MnSe nanostructures increases with the substitution of Cr atoms and the band gap slightly increases with the substitution of Te atoms in MnSe nanostructures. For narrow gap, the electrons easily transit from the valence band to the conduction band owing to substitution of Cr atom in pure MnSe nanostructure. Interestingly, for MnSe nanotube, the conductivity decreases with the substitution of Cr and Te atoms. The corresponding HOMO-LUMO gap values of pure, Cr and Te substituted MnSe nanotube are found to be 3.65, 7.49 and 3.9 eV. Thus, it is inferred that the geometric structure and substitution impurity plays a major role in deciding the conductivity of MnSe nanostructure. Visualization of HOMO-LUMO gap and the density of states spectrum (DOS) for MnSe nanostructures are shown in Table 2.

MnSe nanostructures exhibit semiconducting behaviour with wide band gap. Besides, more energy is required to move the electrons from the valence band to the conduction band. From the observation of DOS spectrum, the localization of charges is observed to be more in LUMO level than in HOMO level. Due to the influence of impurity, the density of charges in both LUMO and HOMO levels gets modified. Thus, the electronic properties of MnSe nanostructures can be tailored with the impurity substitution of Cr and Te atoms.

Table 2. HOMO –LUMO gap and density of states of MnSe nanostructures

Nanostructures	HOMO – LUMO Visualization ■ HOMO ■ LUMO	E_g (eV)	HOMO, LUMO and DOS Spectrum
Pure MnSe nanosheet		3.87	
Cr substituted MnSe nanosheet		2.07	
Te substituted MnSe nanosheet		4.01	



3.1. Ionization potential, electron affinity, chemical potential and chemical hardness of MnSe nanostructures

The electronic properties of MnSe nanostructure can also be discussed with ionization potential (IP) and electron affinity (EA) [31, 32]. Figure 2 depicts the IP and EA of MnSe nanostructures. The amount of energy required for removing the electron from MnSe nanostructure is called as IP and the change in energy due to addition of electrons in MnSe nanostructure is known as EA. Different trends are observed for both IP and EA as shown in Figure 2.

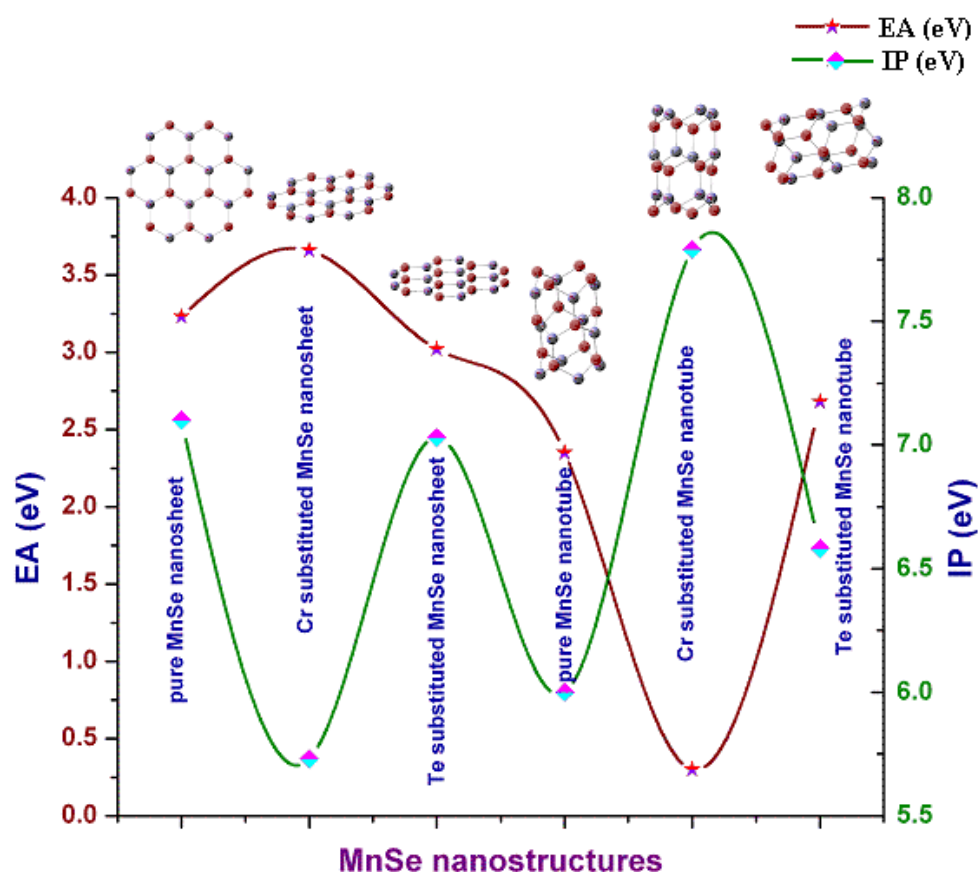


Figure 2. IP and EA of MnSe nanostructures

Electron affinity plays a vital role on both chemical sensors and plasma physics. The EA value of pure, Cr and Te substituted MnSe nanosheet are 3.23, 3.66 and 3.02 eV respectively. The corresponding EA values of pure, Cr and Te substituted MnSe nanotube are 2.35, 0.3 and 2.68 eV.

Table 3. Chemical potential and chemical hardness of MnSe nanostructures

Nanostructures	Chemical potential (eV)	Chemical hardness (eV)
Pure MnSe nanosheet	-5.17	1.94
Cr substituted MnSe nanosheet	-4.7	1.04
Te substituted MnSe nanosheet	-5.03	2.01
Pure MnSe nanotube	-4.16	1.83
Cr substituted MnSe nanotube	-4.05	3.75
Te substituted MnSe nanotube	-4.63	1.95

The structural stability of MnSe nanostructures can also be discussed in terms of chemical harness and chemical potential [33-36]. Chemical potential and chemical hardness can be calculated using the equation $\mu = -(\text{IP} + \text{EA})/2$ and $\eta = (\text{IP} - \text{EA})/2$ respectively as shown in Table 3. The effect of CP and CH can also be revealed by effective fragment potential model. In some cases, the CH can also be represented by electronegativity, which is one of the important factors in semiconductor physics. Almost same CP values in the range of -4.05 to -5.17 eV are observed for MnSe nanostructures. Moreover, only small variations in chemical hardness are found for MnSe nanostructures. In particular, Cr substituted nanotubes have high value of CH, which is 3.75 eV. In contrast, Cr substituted MnSe nanosheet shows a low value of CH as 1.04 eV. This clearly confirms that the geometry of MnSe nanostructure plays an important role in CH. Thus, the structural stability of MnSe nanostructure mainly depends on the substitution of Cr atoms, which is one of the prominent foreign atoms in MnSe nanostructures.

CONCLUSION

The realistic structures of pure, Cr and Te substituted MnSe nanostructures are successfully simulated using B3LYP/LanL2DZ basis set. The structural stability of MnSe nanostructures are studied using calculated energy,

chemical potential and chemical hardness. Dipole moment and point symmetry group of pure, Cr and Te substituted MnSe nanostructures are also reported. Using ionization potential, electron affinity, DOS and HOMO-LUMO gap, the electronic properties of MnSe nanostructures are discussed. From the results of the present work, MnSe nanostructures can be tailored by substituting Cr and Te atoms as dopant elements. Furthermore, structural stability and electronic properties of both nanotube and nanosheet form of MnSe nanostructure can be fine-tuned, which find its potential application in spintronic devices, solar cells and electrocatalysts.

REFERENCES

- [1] S.G. Kwon, T. Hyeon, *Acc. Chem. Res.*, **2008**, 41, 1696.
- [2] P. Johari, V.B. Shenoy, *ACS Nano.*, **2012**, 6, 5449.
- [3] D.S. Wang, W. Zheng, C.H. Hao, Q. Peng, Y.D. Li, *Chem. Eur. J.*, **2009**, 15, 1870.
- [4] H.M. Weng, J.M. Dong, T. Fukumura, M. Kawasaki, Y. Kawazoe, *Phys. Rev. B.*, **2008**, 77, 125206.
- [5] P.A. Chate, P.P. Hankare, D.J. Sathe, *J. Alloys Comp.*, **2010**, 505, 140.
- [6] M.R. Gao, J. Jiang, S.H. Yu, *Small.*, **2012**, 8, 13.
- [7] J.A. Hansen, R. Mukhopadhyay, J.Ø. Hansen, K.V. Gothelf, *J. Am. Chem. Soc.*, **2006**, 128, 3860.
- [8] M.R. Gao, Y.F. Xu, J. Jiang, S.H. Yu, *Chem. Soc. Rev.*, **2013**, 42, 2986.
- [9] R. Lindsay, *Phys. Rev.*, **1951**, 84, 569.
- [10] J.J. Banewicz, R.F. Haidelberg, A.H. Luxem, *J. Phys. Chem.*, **1961**, 65, 615.
- [11] P.W. Anderson, *Phys. Rev.*, **1950**, 79, 705.
- [12] V. Thanigaimani, M.A. Angadi, *Thin Solid Films*, **1994**, 245, 146.
- [13] M. Wu, Y. Xiong, N. Jiang, M. Niang, Q. Chen, *J. Cryst. Growth.*, **2004**, 262, 567.
- [14] M.Z. Xue, Z.W. Fu, *Solid State Ionics.*, **2007**, 178, 273.
- [15] D. Norris, N. Yao, F. Charnock, T. Kennedy, *Nano Lett.*, **2001**, 1, 3.
- [16] L. Levy, N. Feltin, D. Ingert, M. Pileni, *Langmuir.*, **1999**, 15, 3386.
- [17] J. Suyver, S. Wuister, J. Kelly, A. Meijerink, *Nano Lett.*, **2001**, 1, 429.
- [18] M. Wu, Y. Xiong, N. Jiang, M. Ning, Q. Chen, *J. Cryst. Growth.*, **2004**, 262, 567.
- [19] H.J. Chun, J.Y. Lee, D.S. Kim, S.W. Yoon, J.H. Kang, J. Park, *J. Phys.Chem.C.*, **2007**, 111, 519.
- [20] S. Lei, K. Tang, H. Zheng, *Mater. Lett.*, **2006**, 60, 1625.
- [21] M.Frisch et al., Gaussian 09, Revision D.01, Gaussian, Inc., Wallingford CT., **2009**.
- [22] R.Chandiramouli, *Res. J. Chem. Environ.*, **2013**, 17, 64.
- [23] V.Nagarajan, R. Chandiramouli, *Int.J. ChemTech Res.*, **2014**, 6(4), 2240.
- [24] V.Nagarajan, R. Chandiramouli, *Alexandria Engineering Journal.*, **2014**, 53, 437.
- [25] R.Srinivasaraghavan, R. Chandiramouli, B.G.Jeyaprakash, S. Seshadri, *Spectrochim. Acta, Part A.*, **2013**, 102, 242.
- [26] N.M.O'boyle, A.L.Tenderholt, K.M.Langner, *J. Comput. Chem.*, **2007**, 29, 839.
- [27] V.Ganesan, V.Nagarajan, V.Saravanakannan, R.Chandiramouli, *Int.J. ChemTech Res.*, **2014**, 6(7), 3832.
- [28] S.Sriram, R.Chandiramouli, D.Balamurugan, A. Thayumanvan, *Eur. Phys. J. Appl. Phys.*, **2013**, 62, 30101.
- [29] V.Nagarajan, V.Saravanakannan, R.Chandiramouli, *Int.J. ChemTech Res.*, **2014**, 6(5), 2962.
- [30] V.Nagarajan, R.Chandiramouli, *Res J Pharm BiolChemSci*, **2014**, 5(1), 365.
- [31] V.Nagarajan, R.Chandiramouli, *Der PharmaChemica.*, **2014**, 6 (1), 37.
- [32] V.Nagarajan, R.Chandiramouli, *Int.J. ChemTech Res.*, **2014**, 6(1), 21.
- [33] R.Chandiramouli, S.Sriram, D.Balamurugan, *Mol. Phys.*, **2014**, 112, 151.
- [34] V.Nagarajan, R.Chandiramouli, S.Sriram, P.Gopinath, *J Nanostruct Chem.*, **2014**, 4, 87.
- [35] S.Sriram, R.Chandiramouli, B.G.Jeyaprakash, *Struct Chem.*, **2014**, 25, 389.
- [36] V.Ganesan, V.Nagarajan, V.Saravanakannan, R.Chandiramouli, *Int.J. ChemTech Res.*, **2014**, 6 (7), 3822.